

## The Electrochemistry of $[\text{PtH}(\text{PEt}_3)_3]^+$ ; Inverted and Amplified Cyclic Voltammetric Waves and Catalytic Hydrogen Production at a Mercury Electrode

Richard G. Compton

Physical Chemistry Laboratory, University of Oxford, South Parks Road, Oxford

David J. Cole-Hamilton\*

Chemistry Department, University of St. Andrews, Fife KY16 9ST

Inverted and amplified waves in cyclic voltammograms of  $[\text{PtH}(\text{PEt}_3)_3]^+$  at a sitting mercury drop electrode are interpreted in terms of catalytic cycles for hydrogen production from water involving adsorbed species. The adsorption step on the cathodic sweep involves a two-electron reduction to the catalytically inactive species  $[\text{PtH}(\text{PEt}_3)_3]^-$  (ads.). On the reverse (anodic) sweep, a reductive catalytic cycle is initiated by oxidation to  $[\text{PtH}(\text{PEt}_3)_3]^+$  (ads.) and stops when the potential is insufficiently negative to reduce  $[\text{Pt}(\text{PEt}_3)_3]^{2+}$  (ads.) {or  $[\text{PtH}_2(\text{PEt}_3)_3]^{2+}$  (ads.)}. In second and subsequent forward scans the catalytic cycle restarts when the potential is sufficiently reducing to reduce  $[\text{Pt}(\text{PEt}_3)_3]^{2+}$  (ads.) or  $[\text{PtH}_2(\text{PEt}_3)_3]^{2+}$  (ads.) and terminates when  $[\text{PtH}(\text{PEt}_3)_3]^+$  (ads.) is reduced to  $[\text{PtH}(\text{PEt}_3)_3]^-$  (ads.). Variations in peak shape and position with  $[\text{PtH}(\text{PEt}_3)_3]^+$  (aq.) concentration are interpreted in terms of partial or full desorption of  $[\text{Pt}(\text{PEt}_3)_3]^{2+}$  (ads.) or  $[\text{PtH}(\text{PEt}_3)_3]^+$  (ads.) during the catalytic cyclic under certain conditions. Catalysis of hydrogen production at a mercury drop electrode with catalyst turnover numbers up to  $2 \times 10^5 \text{ h}^{-1}$  for  $> 16 \text{ h}$  is also described.

Inverted peaks, which are often correlated with polarographic maxima have been observed in cyclic voltammograms of a range of different materials and generally take the form of reduction waves observed during the anodic sweep of the cyclic voltammogram.<sup>1-9</sup>

The most common substrates for which these features are observed are alkyl halides<sup>5-9</sup> or 'onium' salts (tetra-alkylammonium, phosphonium or sulphonium),<sup>1-4</sup> which, in their reduced form may be capable of forming amalgams with the mercury drop electrode.<sup>1-4, 10-14</sup> In these cases, it has been proposed that amalgam formed during the cathodic sweep increases the overpotential for the reduction of the onium salt from solution before all of the species in the diffusion layer has been reduced. On the reverse sweep, the amalgamated anion radical is oxidised at a potential more negative than that required for reduction of the free onium salt so that any unreduced onium salt in the diffusion layer will be reduced despite the fact that an anodic sweep is taking place. It has also been suggested that a two-electron reduction of the onium ion may be important.<sup>4</sup>

For alkyl halides, the inverted peaks are also usually attributed to amalgam formation, this occurring by chemical reduction of the supporting electrolyte by radicals or diradicals derived from the alkyl halide.<sup>8</sup>

Ginzburg *et al.*<sup>14</sup> have, however, suggested that all of these phenomena can be interpreted in terms of physical rather than chemical phenomena. These physical phenomena include inhomogeneous polarisation of the mercury drop, which is probable only in non-aqueous media, and/or an inhomogeneous adsorption of a surface active species. These inhomogeneities lead to differences in surface tension over the drop surface and hence to vibrations of the drop and stirring of the solution adjacent to the mercury drop; these vibrations account for the irregular or inverted peaks observed.

These explanations are clearly plausible in a number of instances; indeed we have shown<sup>15</sup> that they are responsible for inverted peaks in the cyclic voltammograms of *e.g.*  $\text{CF}_3\text{CHBrCl}$ ,

but the observation<sup>16</sup> of inverted waves in cyclic voltammograms of  $\text{HCO}(\text{OH})$  or  $\text{CH}_2\text{O}$  at a (solid) platinum electrode clearly cannot be explained in this way. In any case, it is generally agreed that adsorption of the substrate in its reduced or oxidised form is responsible for these inverted maxima.

During the course of extensive studies into the use of low-valent platinum metal hydrides for hydrogen production from water<sup>17-21</sup> or alcohols,<sup>22</sup> we have investigated the electrochemistry of  $[\text{PtH}(\text{PEt}_3)_3]^+$  at a mercury drop electrode.

In cyclic voltammograms of this complex we have observed inverted waves, but unlike those previously observed, these maxima show very substantial amplification relative to normal diffusion controlled processes. We now report details of these studies, for which a preliminary communication has been published.<sup>23</sup>

### Results and Discussion

A d.c. cyclic voltammogram of  $[\text{PtH}(\text{PEt}_3)_3]^+$  ( $1.5 \times 10^{-4} \text{ mol dm}^{-3}$ ) in phosphate buffer ( $0.5 \text{ mol dm}^{-3}$ , pH 6.88) is shown in Figure 1. In the first scan [Figure 1(a)] there are only two very small reductive waves (A and B) during the cathodic sweep, prior to breakdown of the solvent. Since reversing the scan before or after wave B leads to identical subsequent scans, it is clear that wave B is not necessary for the chemistry of the subsequent scans and it will, therefore, be ignored during the following discussion.

The first anodic scan shows a large approximately Gaussian reductive (*i.e.* inverted) wave (C) with a maximum at *ca.*  $-1.5 \text{ V}$ . The second cathodic scan [Figure 1(b)] also shows a similar large reductive wave, D, at *ca.*  $-1.6 \text{ V}$ . Subsequent cathodic and anodic scans are identical to those shown in Figure 1(b). Hydrogen production (bubbles) is observed during passage of waves C and D.

As pointed out above, inverted and amplified waves can often be explained<sup>14</sup> in terms of oscillations of mercury drops caused by inhomogeneous coverage of the drop surface during ad-

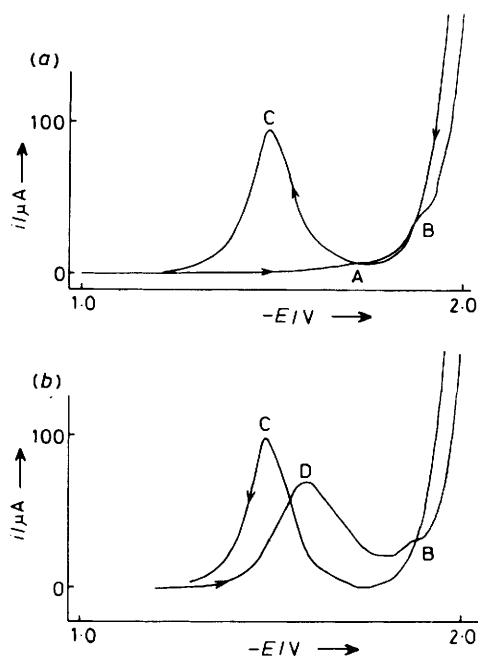


**Figure 1.** Cyclic voltammograms of  $[\text{PtH}(\text{PEt}_3)_3]^+$  ( $1.5 \times 10^{-4}$  mol  $\text{dm}^{-3}$ ) at a mercury drop electrode. (a) first scan; (b) second and subsequent scans. For peak assignments see text. Scan rate  $100 \text{ mV s}^{-1}$

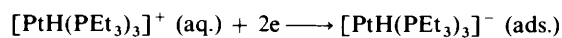
sorption or desorption processes. Certainly, drop oscillations do occur during the passage of waves C and D since vigorous hydrogen evolution is observed; however, we can show that these oscillations are not responsible for the inversion or amplification since identical cyclic voltammograms are obtained using a copper wire plated with a thin layer of mercury. Such electrodes have been shown<sup>24</sup> to be quantitatively identical to sitting mercury drop electrodes. Furthermore, the height of waves C and D is proportional to the length of mercury-plated copper wire immersed in the solution, confirming that vibrations of a mercury drop are not a prerequisite for the observed inverted and amplified waves.

We offer the following chemical explanation of the observed cyclic voltammetric behaviour of  $[\text{PtH}(\text{PEt}_3)_3]^+$ . Subsequently we discuss the effects of scan rate and changing concentration of  $[\text{PtH}(\text{PEt}_3)_3]^+$  on the shapes and positions of each wave in turn, which support this chemical explanation.

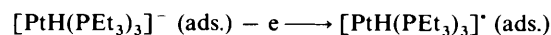
We believe that wave A represents a two-electron reduction of  $[\text{PtH}(\text{PEt}_3)_3]^+$  (aq.) which leads to an adsorbed monolayer of  $[\text{PtH}(\text{PEt}_3)_3]^-$  (ads.). This species is not active for hydrogen production but remains on the electrode throughout the remainder of the first negative scan and the first positive scan until the potential is sufficient to induce the one-electron oxidation of  $[\text{PtH}(\text{PEt}_3)_3]^-$  (ads.) to the radical  $[\text{PtH}(\text{PEt}_3)_3]^\cdot$  (ads.). This radical is then catalytically active for hydrogen production as shown in the Scheme and, since this reaction is reductive, an inverted wave, C, is observed. The catalytic reaction proceeds at a high rate until the potential is insufficiently reducing to drive one of the reduction reactions, at which point the hydrogen production switches off, accounting for the approximately Gaussian shape of wave C.

Since a platinum species is still adsorbed on the electrode surface, by scanning negatively the catalytic cycle can be switched on again as soon as the potential is sufficiently negative to drive both reduction reactions of the catalytic cycle and hence a large reductive wave (D) is observed on all subsequent cathodic scans. The catalytic reaction proceeds until the

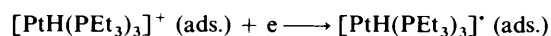
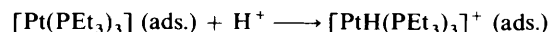
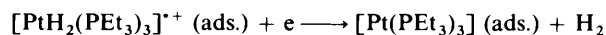
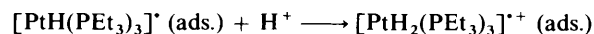
(i) Adsorption



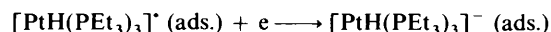
(ii) Initiation



(iii) Catalytic cycle



(iv) Termination



**Scheme.** Proposed reactions occurring during cyclic voltammograms of  $[\text{PtH}(\text{PEt}_3)_3]^+$  at a mercury drop electrode in aqueous phosphate buffer ( $0.5 \text{ mol dm}^{-3}$ , pH 6.88)

potential is sufficiently negative for reduction of  $[\text{PtH}(\text{PEt}_3)_3]^\cdot$  (ads.) to the catalytically inactive  $[\text{PtH}(\text{PEt}_3)_3]^-$  (ads.) to occur. Hydrogen production switches off and a Gaussian shape for wave D is also observed. These reactions are summarised in the Scheme.

The inversion of wave C can then be attributed to an oxidative initiation of a reductive catalytic cycle whilst the amplification of waves C and D are attributable to catalytic hydrogen production.

**Wave A.**—The shape of wave A changes from the very diffuse feature shown in Figure 1(a) to a much sharper feature as the concentration of  $[\text{PtH}(\text{PEt}_3)_3]^+$  (aq.) is increased from  $1.5 \times 10^{-4}$  to  $4 \times 10^{-4}$  mol  $\text{dm}^{-3}$ . This is consistent with the reductive deposition of a controlled amount of an adsorbed species since, at low concentrations, material will have to diffuse from considerable distances from the electrode, whilst at higher concentrations more material will be available close to the electrode and saturation coverage will occur more quickly, giving a Gaussian shape.

The area of wave A, measured at a higher concentration of  $[\text{PtH}(\text{PEt}_3)_3]^+$  (aq.), corresponds to the passage of  $5 \times 10^{-6}$  Coulombs for a drop with a diameter of 1 mm.

Assuming that the area of a molecule of  $[\text{PtH}(\text{PEt}_3)_3]^+$  is  $20 \text{ \AA}^2$ , one monolayer on a 1 mm drop should contain  $1.5 \times 10^{13}$  molecules.

Clearly then, the area of wave A can be attributed to the formation of a monolayer of  $[\text{PtH}(\text{PEt}_3)_3]^-$  (ads.) by a two-electron reduction of  $[\text{PtH}(\text{PEt}_3)_3]^+$ . We cannot, however, on this basis strictly rule out the possibility of a one-electron reduction leading to a layer two molecules thick.

**Wave C.**—(a) *Scan rate dependence.* At low solution concentrations of  $[\text{PtH}(\text{PEt}_3)_3]^+$  (aq.), the shape of wave C is almost independent of scan rate, although its position varies.

At higher concentrations of  $[\text{PtH}(\text{PEt}_3)_3]^+$  (aq.), however, this is not the case. At high scan rates [Figure 2(a)] wave C has a Gaussian shape, whilst at lower scan rates there is a more rapid reduction in current on the positive side of the wave [see Figure 2(b) and (c)]. The probable explanation for this change in shape at low scan rates is that some species is desorbing from the surface of the drop during the catalytic cycle causing a rapid

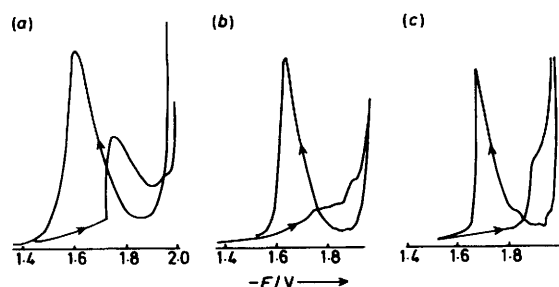


Figure 2. Dependence of the shape of wave C upon scan rate in cyclic voltammograms of  $[\text{PtH}(\text{PEt}_3)_3]^+$  ( $4 \times 10^{-4} \text{ mol dm}^{-3}$ ): (a) 100, (b) 50, and (c)  $20 \text{ mV s}^{-1}$

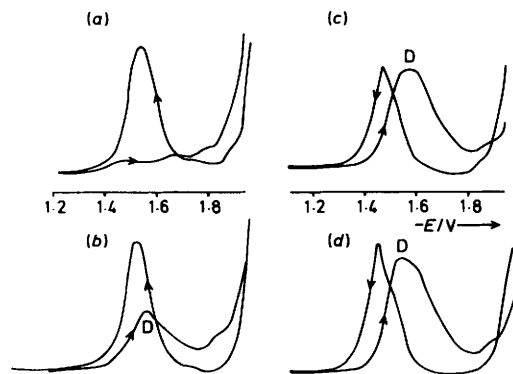


Figure 3. Dependence of wave D upon scan rate in cyclic voltammograms of  $[\text{PtH}(\text{PEt}_3)_3]^+$  ( $10^{-4} \text{ mol dm}^{-3}$ ): (a) 20, (b) 50, (c)  $100 \text{ mV s}^{-1}$ , (d)  $100 \text{ mV s}^{-1}$  held for 120 s at  $-0.4 \text{ V}$  prior to cathodic scan

reduction in the rate of the catalytic reaction. The nature of this desorbing species is discussed below.

(b) *Concentration dependence.* The height of wave C varies with concentration. Thus, at low concentrations the wave height increases with increasing  $[\text{PtH}(\text{PEt}_3)_3]^+$  (aq.) concentration. This is consistent with the partial coverage of the electrode surface, as deduced from the charge passed during wave A (see above). From  $ca. 2.5 \times 10^{-4}$  to  $5 \times 10^{-4} \text{ mol dm}^{-3}$  the peak height remains approximately constant, as expected for monolayer coverage, but it drops again at higher  $[\text{PtH}(\text{PEt}_3)_3]^+$  (aq.) concentrations. This is presumably because the potential of desorption ( $E_{\text{des.}}$ ) is more negative than that of the peak maximum ( $E_{\text{max.}}$ ). Finally, at higher concentrations of  $[\text{PtH}(\text{PEt}_3)_3]^+$  (aq.) ( $> 2 \times 10^{-3} \text{ mol dm}^{-3}$ ), wave C is not observed since  $E_{\text{des.}}$  is now more negative than the onset potential of wave C.

One other point of interest is that the area of wave C is some 250 times that of wave A, suggesting highly efficient catalysis of the hydrogen producing reaction. We shall return to this subject below.

*Wave D.*—(a) *Scan rate dependence.* Cyclic voltammograms of  $[\text{PtH}(\text{PEt}_3)_3]^+$  at different scan rates are illustrated in Figure 3. These clearly show that the height of wave D is highly sensitive to scan rate, being similar to that of wave C at high scan rate ( $100 \text{ mV s}^{-1}$ ) but almost non-existent at lower scan rates ( $20 \text{ mV s}^{-1}$ ). Such a dramatic transition as the scan rate is altered by merely a factor of 5 is utterly inconsistent with a purely diffusional process and, as also deduced from the behaviour of wave C (see above), must be rationalised in terms of desorption of some species during wave C. That the desorption occurs during the passage of wave C and that the

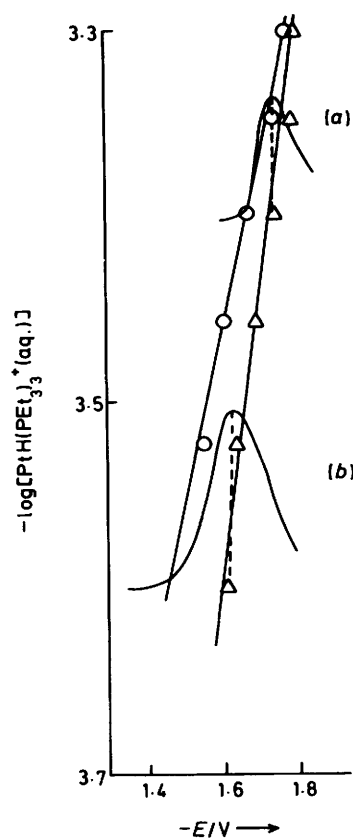


Figure 4. Plot of  $\log [\text{PtH}(\text{PEt}_3)_3^+ (\text{aq.})]$  against wave maximum  $E'_{\text{max.}}$  ( $\Delta$ ) and start of wave  $E_{\text{ads.}}$  ( $\circ$ ) for wave D, scan rate =  $100 \text{ mV s}^{-1}$ . Superimposed are wave D at  $[\text{PtH}(\text{PEt}_3)_3^+]$  of (a)  $4 \times 10^{-4}$ , and (b)  $2.5 \times 10^{-4} \text{ mol dm}^{-3}$

desorbing species is *not* the species present on the surface at potentials less negative than  $-1.3 \text{ V}$  is confirmed by Figure 3(d). In this voltammogram, the scan was stopped for 120 s at  $-0.4 \text{ V}$  after the positive scan before scanning negatively. The presence of wave D in this scan shows that no desorption occurs during the holding at  $-0.4 \text{ V}$ . Once again we conclude that desorption occurs during the catalytic cycle.

(b) *Concentration dependence.* The concentration dependence of wave D is shown in Figure 4. First, the position of the maximum changes with the concentration of  $[\text{PtH}(\text{PEt}_3)_3]^+$  (aq.) and secondly the shape of the wave varies. At concentrations below  $3 \times 10^{-4} \text{ mol dm}^{-3}$  (where  $E_{\text{ads.}} > E_{\text{thresh.}}$ , the onset potential for wave D) the position of the wave is essentially concentration independent. Thus, at scan rates of  $100 \text{ mV s}^{-1}$  and concentrations below  $3 \times 10^{-4} \text{ mol dm}^{-3}$ , wave D has an approximately Gaussian shape. Between  $3 \times 10^{-4}$  and  $5 \times 10^{-4} \text{ mol dm}^{-3}$  of  $[\text{PtH}(\text{PEt}_3)_3]^+$  the wave has an abrupt beginning and above  $ca. 5 \times 10^{-4} \text{ mol dm}^{-3}$  wave D disappears.

We interpret these phenomena in terms of readsorption of the species that desorbs during the passage of wave C. At low concentration, the potential for readsorption ( $E_{\text{ads.}}$ ) is less negative than that of the onset of wave D ( $E_{\text{thresh.}}$ ) and hence a Gaussian wave is observed. In the intermediate region,  $E_{\text{ads.}}$  lies between the potential of the maximum ( $E'_{\text{max.}}$ ) and  $E_{\text{thresh.}}$ , whilst at higher concentrations  $E_{\text{ads.}} < E'_{\text{max.}}$ .

*The Natures of the Desorbing Species and the Species present at  $> -1.3 \text{ V}$ .*—*Species present at  $> -1.3 \text{ V}$ .* Certain of the observations described above make it possible to identify the

species present on the surface at more positive potentials than  $-1.3$  V. We have shown above that wave A corresponds to the reduction of  $[\text{PtH}(\text{PEt}_3)_3]^+$  from solution. Thus, since implicit in the mechanism (Scheme) is the idea that adsorbed  $[\text{PtH}(\text{PEt}_3)_3]^+$  is more readily reduced than the solution species, we must conclude that  $[\text{PtH}(\text{PEt}_3)_3]^+$  does not adsorb from solution at potentials positive of *ca.*  $-1.8$  V. Hence the species present at potentials positive of  $-1.3$  V cannot be  $[\text{PtH}(\text{PEt}_3)_3]^+$ . Similarly, since the protonation reactions of the catalytic cycle are extremely rapid, the species present at  $-1.3$  V cannot be  $[\text{Pt}(\text{PEt}_3)_3]$  (ads.), since this would protonate and desorb. We can also rule out  $[\text{PtH}(\text{PEt}_3)_3]^-$  (ads.) as the species present at  $-1.3$  V since, in order to start the catalytic cycle of wave D, the species present must undergo reduction.  $[\text{PtH}(\text{PEt}_3)_3]^-$  (ads.) would, however, give the non-catalytically active  $[\text{PtH}(\text{PEt}_3)_3]^-$  (ads.) on reduction. This means that the species present at higher applied potentials must be  $[\text{PtH}_2(\text{PEt}_3)_3]^{2+}$  (ads.) or  $[\text{Pt}(\text{PEt}_3)_3]^{2+}$  (ads.). We favour the latter since all the reactions in the catalytic cycle are rapid and hence  $[\text{PtH}_2(\text{PEt}_3)_3]^{2+}$  (ads.) would rapidly produce  $[\text{Pt}(\text{PEt}_3)_3]^{2+}$  (ads.) (loss of hydrogen from the  $\text{Pt}^{\text{III}}$  dihydride would be expected to be rapid by comparison with the  $\text{Pt}^{\text{II}}$  dihydride and would probably precede reduction in the catalytic cycle, although we cannot be certain of this).

It is possible to deduce that the reduction that requires the more negative potentials and is the rate-determining step on the positive side of waves C and D must be that of  $[\text{Pt}(\text{PEt}_3)_3]^{2+}$  (ads.) {or  $[\text{PtH}_2(\text{PEt}_3)_3]^{2+}$  (ads.)}. The rate-determining step on the negative side of these waves is the relevant reaction of the redox couple  $[\text{PtH}(\text{PEt}_3)_3]^- / ^+$  (ads.). Interestingly, diffusion-controlled processes never become rate determining in the catalytic waves.

*The species desorbing during the catalytic cycle.* Clearly the species which desorbs cannot be  $[\text{Pt}(\text{PEt}_3)_3]^{2+}$  or  $[\text{PtH}_2(\text{PEt}_3)_3]^{2+}$  since these are the major species present at less negative potentials and do not desorb.  $[\text{PtH}(\text{PEt}_3)_3]^+$  cannot be the desorbing species since it would not re-adsorb during wave D. The desorbing species must, therefore, be  $[\text{Pt}(\text{PEt}_3)_3]$  or  $[\text{PtH}(\text{PEt}_3)_3]^-$ . We favour the former since the radical is likely to be covalently bound to the surface and since at high concentration of  $[\text{PtH}(\text{PEt}_3)_3]^+$  (aq.), where desorption occurs as  $[\text{PtH}(\text{PEt}_3)_3]^-$  (ads.) is oxidised, it is possible to see an orange colour around the drop similar to the known colour of  $[\text{Pt}(\text{PEt}_3)_3]$ .<sup>26</sup> Clearly,  $[\text{Pt}(\text{PEt}_3)_3]$  should protonate since it does very rapidly during the catalytic cycle. However, in water the protonation reaction is slow, largely because  $[\text{Pt}(\text{PEt}_3)_3]$  is an orange oil which is immiscible with water.<sup>25</sup>

*Possible Alternative Mechanism.*—One other possible mechanism does appear to fit the observations described above. It requires that wave A corresponds to a one-electron reduction of  $[\text{PtH}(\text{PEt}_3)_3]^+$  (aq.) to give an adsorbed layer of square planar  $[\text{PtH}(\text{PEt}_3)_3]^-$  (ads.) standing on its edge. In this state it is not catalytically active. However, on the first anodic scan,  $[\text{PtH}(\text{PEt}_3)_3]^-$  (ads.) starts to desorb and the remaining molecules lie down flat on the surface since there is more space available to them. In this state, they are more strongly adsorbed and catalytically active for hydrogen production. The remaining phenomena can then be described by the same catalytic cycle as discussed above but the switching off of wave D occurs because  $[\text{PtH}(\text{PEt}_3)_3]^+$  (aq.) reduces and adsorbs forcing the molecules on the surface of the drop to stand up again. Similar potential driven changes of adsorption mode between parallel with and perpendicular to the surface have been observed for *e.g.* aniline on a mercury drop electrode.<sup>27</sup>

However, at low concentrations of  $[\text{PtH}(\text{PEt}_3)_3]^+$  (aq.) we believe that only partial coverage of the drop occurs (see above), we would thus expect some molecules to be flat on the surface at

highly negative potentials and hence hydrogen production should be observed. Since this is not the case, we do not favour this explanation for the observed features of the cyclic voltammograms.

*Catalytic Hydrogen Production.*—By sweeping anodically to  $-1.7$  V on wave C and potentiostating, it is possible to observe catalytic hydrogen production over a period of at least 16 h. Provided that the solution is stirred continuously at a  $[\text{PtH}(\text{PEt}_3)_3]^+$  (aq.) concentration of  $2.5 \times 10^{-4}$  mol dm<sup>-3</sup>, a constant current of *ca.* 250  $\mu\text{A}$  can be passed by a 1-mm diameter Hg drop. Assuming monolayer coverage, this corresponds to an extremely efficient catalytic reaction with a catalyst turnover number of  $\sim 2 \times 10^5$  h<sup>-1</sup>.

## Experimental

Cyclic voltammograms were obtained using an Oxford Electrodes potentiostat with a linear sweep capability in a three compartment cell with a sitting mercury drop (radius  $\approx 0.5$  mm) or mercury-plated copper wire working electrode, a platinum gauze secondary electrode and a saturated calomel (s.c.e.) reference electrode. The electrolyte (triply distilled water) had a volume of 40 cm<sup>3</sup>. The supporting electrolyte was  $\text{Na}_2\text{HPO}_4$  (0.25 mol dm<sup>-3</sup>) and  $\text{KH}_2\text{PO}_4$  (0.25 mol dm<sup>-3</sup>) which also acted as a buffer at pH 6.9.

$[\text{Pt}(\text{PEt}_3)_3]$  was prepared by a standard literature<sup>26</sup> method and dissolved in the above buffer to give a solution of  $[\text{PtH}(\text{PEt}_3)_3]^+$  ( $3.8 \times 10^{-2}$  mol dm<sup>-3</sup>, determined gravimetrically).<sup>19</sup> Aliquots of this solution (typically 0.05 cm<sup>3</sup>) were added to the electrolyte to vary the concentration of  $[\text{PtH}(\text{PEt}_3)_3]^+$ . All electrochemical studies were carried out on degassed solutions under nitrogen. All potentials are quoted relative to the saturated calomel electrode.

*Sustained Catalytic Hydrogen Production.*—A solution of  $[\text{PtH}(\text{PEt}_3)_3]^+$  ( $2.5 \times 10^{-4}$  mol dm<sup>-3</sup>) was placed in the cell described above. The applied voltage was swept anodically to  $-1.7$  V and potentiostated. The solution was stirred by bubbling with nitrogen. A continuous current of 250  $\mu\text{A}$  was drawn from the drop for 1 h without noticeable reduction and catalytic hydrogen production (bubbles) was still occurring after 16 h.

## Acknowledgements

We thank Johnson Matthey p.l.c. for generous loans of platinum metals and Drs. G. Sealy and J. Fisher for some preliminary experiments. D. J. C-H. is Sir Edward Frankland Fellow of the Royal Society of Chemistry 1984—1985.

## References

- 1 D. A. Tyssee, *J. Electroanal. Chem.*, 1971, **30**, App. 14.
- 2 D. A. Tyssee and M. M. Baizer, *J. Electrochem. Soc.*, 1971, **118**, 1420.
- 3 J. M. Saveant and S. K. Binh, *J. Org. Chem.*, 1977, **42**, 1242.
- 4 E. A. H. Hall and L. Horner, *Ber. Bunsenges. Phys. Chem.*, 1980, **84**, 1145.
- 5 B. Fleet and R. D. Jee, *J. Electroanal. Chem.*, 1970, **25**, 397.
- 6 P. Tissot and P. Margaretha, *Electrochim. Acta*, 1978, **23**, 1049.
- 7 P. Margaretha and P. Tissot, *J. Electroanal. Chem.*, 1979, **99**, 127.
- 8 P. Tissot and P. Margaretha, *Helv. Chim. Acta*, 1981, **64**, 180.
- 9 D. M. La Perriere, W. F. Carroll, B. C. Willett, E. C. Torp, and D. G. Peters, *J. Am. Chem. Soc.*, 1979, **101**, 7561.
- 10 J. D. Littlehailes and B. J. Woodhall, *Chem. Commun.*, 1967, 665.
- 11 J. Myatt and P. F. Todd, *Chem. Commun.*, 1967, 1033.
- 12 W. R. T. Cottrell and R. A. N. Morris, *Chem. Commun.*, 1968, 409.
- 13 J. Kariv-Miller and C. Nanjudiah, *J. Electroanal. Chem.*, 1983, **147**, 319.

- 14 G. Ginzburg, J. Y. Becker, and E. Lederman, *Electrochim. Acta*, 1981, **26**, 851.
- 15 M. P. Ellerby and R. G. Compton, unpublished work.
- 16 R. R. Advic, A. V. Tripkovic, and W. E. O'Grady, *Nature (London)*, 1982, **296**, 137.
- 17 R. F. Jones and D. J. Cole-Hamilton, *J. Chem. Soc., Chem. Commun.*, 1981, 58.
- 18 R. F. Jones and D. J. Cole-Hamilton, *J. Chem. Soc., Chem. Commun.*, 1981, 1245.
- 19 R. F. Jones, J. R. Fisher, and D. J. Cole-Hamilton, *J. Chem. Soc., Dalton Trans.*, 1981, 2550.
- 20 D. J. Cole-Hamilton, R. F. Jones, J. R. Fisher, and D. W. Bruce 'Photogeneration of Hydrogen,' eds. A. Harriman and M. A. West, Academic Press, London, 1982, p.105.
- 21 J. R. Fisher and D. J. Cole-Hamilton, *J. Chem. Soc., Dalton Trans.*, 1984, 809.
- 22 E. Delgado-Leita, M. A. Luke, and R. F. Jones, *Polyhedron*, 1982, **1**, 839.
- 23 J. R. Fisher, R. G. Compton, and D. J. Cole-Hamilton, *J. Chem. Soc., Chem. Commun.*, 1983, 555.
- 24 P. J. Daly, D. J. Page, and R. G. Compton, *Anal. Chem.*, 1983, **55**, 119.
- 25 D. H. Gerlach, A. R. Kane, G. W. Parshall, J. P. Jesson, and E. L. Muetterties, *J. Am. Chem. Soc.*, 1971, **93**, 3543.
- 26 R. A. Schunn, *Inorg. Chem.*, 1976, **15**, 208.
- 27 E. Blomgen, J. O'M. Bockris, and G. Jesch, *J. Phys. Chem.*, 1961, **65**, 2000.

Received 26th July 1985; Paper 5/1279